Lepton nonconservation at supercollider energies

Duane A. Dicus and Debra Dzialo Karatas
Center for Particle Theory, University of Texas at Austin, Austin, Texas 78712

Probir Roy*
Physics Department, University of Texas at Austin, Austin, Texas 78712
(Received 25 March 1991)

The lepton-nonconserving rare process $pp \to (\text{jet})_1(\text{jet})_2 e^+ e^+$, without missing p_T, is the high-energy analog of neutrinoless nuclear double-β decay. It is shown to be a possible signal to search for a heavy Majorana electronlike neutrino N_e in the mass intervals 150–1400 GeV and 450–1700 GeV at the CERN Large Hadron Collider (LHC) and the Superconducting Super Collider, respectively, with event rates of a few per year. However, standard-model backgrounds probably preclude seeing this process at the LHC.

Neutrinos are the only charge neutral elementary fermions known today. With a possible nonzero mass any one of them could have a Majorana [1] character, i.e., have two independent spinorial components, with the particle and antiparticle being identical. Such particles need not be light; heavy Majorana neutrinos could exist and, as discussed below, there has been much theoretical speculation concerning them. In this paper we propose an experimental signature for a heavy ($\sim$ TeV) electronlike Majorana neutrino. Such an object can mediate the lepton-nonconserving high-energy reaction $pp \to (\text{jet})_1(\text{jet})_2 e^+ e^+$. We shall evaluate the cross section for this process (within practicable cuts) at c.m. energies of 16 and 40 TeV for the CERN Large Hadron Collider (LHC) and the Superconducting Super Collider (SSC), respectively, and discuss the corresponding ranges of the Majorana mass that can be probed.

We have a largely exploratory motivation behind our effort. The reaction of our interest is the high-energy analog of neutrinoless nuclear double-β decay; in fact, the subprocess diagrams are very similar. The latter is a low-energy process that has been experimentally investigated for several nuclei. Its lack of observation has ruled out an electron neutrino of Majorana mass between ~ 1 eV and 2 GeV [2]. The high-energy analog also should be studied. As we shall see, the cross section (for any possible range of the Majorana mass) is too small to be measured at TeV or sub-TeV energies. It begins to be interesting only in the multi-TeV region, i.e., with respect to the forthcoming LHC and SSC machines where a Majorana mass ~ 1 TeV can be probed.

There could be several heavy Majorana neutrinos, all mixing with the standard-model neutrino. Let us confine ourselves to the lowest generation for the moment. If N_{ej} stands for the jth physical Majorana neutrino with mass eigenvalue M_j, the weak eigenstate ν_{eL} appearing in the gauge interactions of the standard model is a complex linear combination of all N_{ej}:

$$|\nu_{eL}\rangle = \sum_{j=0} U_{ej} |N_{ej}\rangle \ . \tag{1}$$

The mixing matrix element U_{ej} therefore appears as a coefficient of the gauge coupling at the vertex where a charged W boson converts e into N_{ej}.

We first take up as a paradigm the simplest lepton-nonconserving reaction that can be mediated by such an N_{ej}, namely $W^+W^+ \to e^+e^+$. (The same remarks pertain to $W^-W^- \to e^-e^-$; however, we are more interested in positively charged W's since they are easier to produce in pp collisions.) The tree-level amplitude, consists of N_{ej} exchanges both in the t and u channels (Fig. 1). Assign four-momenta r_1, r_2 to the incident W's and p_3, p_4 to the final positrons. The invariant amplitude can now be written in terms of the $SU(2)_L$ gauge coupling strength g as

$$\hat{\mathcal{M}}_j = \left[\frac{g}{\sqrt{2}}\right]^2 M_j U_{ej}^2 \bar{u}(p_3) \left[\frac{\gamma_\mu \frac{1}{2}(1-\gamma_5)\gamma_\nu}{\hat{t}-m_j^2} + \frac{\gamma_\nu \frac{1}{2}(1-\gamma_5)\gamma_\mu}{\hat{u}-M_j^2} \right] v(p_4) \ . \tag{2}$$

In (2) we have defined $\hat{t} \equiv (p_3 - r_1)^2 = M_W^2 - 2p_3 \cdot r_1$, $\hat{u} \equiv (p_3 - r_2)^2 = M_W^2 - 2p_3 \cdot r_2$ and $\hat{s} \equiv (r_1 + r_2)^2 = 2M_W^2 + 2r_1 \cdot r_2$, ignoring the positron mass. The corresponding differential cross section with respect to the c.m. scattering angle θ in the limit of large $\hat{s}$ is

$$\lim_{\hat{s}\to\infty} \frac{d\hat{\sigma}}{d\cos\theta} = \frac{g^4}{144\pi} \frac{1}{M_W^4} \left| \sum_j U_{ej}^2 M_j \right|^2 + O\left[\frac{M_W^2}{\hat{s}}, \frac{M_j^2}{\hat{s}} \right] . \tag{3}$$

Thus the violation of tree unitarity at large $\hat{s}$, implied by the first right-hand side (RHS) term in (3), gets cured if

$$\sum_j U_{ej}^2 M_j = 0 \ . \tag{4}$$

A similar analysis for the reaction $e^-e^- \to W^-W^-$ had earlier been done [3] by Rizzo. However, he had considered the exchange of a single heavy Majorana neu-

trino so that (4) could not be satisfied. Reference [3] had a Higgs triplet carrying lepton number 2 whose neutral component would generate the Majorana mass through a vacuum expectation value (VEV). The exchange of a doubly charged member of this triplet in the $\hat{s}$ channel restored the high-energy unitarity of the tree amplitude for $e^-e^-\to W^-W^-$. However, a light Majoron and a not particularly heavy scalar are generic to models in which a Higgs triplet carries a nonzero lepton number and has a rather small VEV from its neutral component to adjust to the right value of M_W/M_Z. Such a pair would play a significant role in Z decay [4]. The most recent data on Z decay from the CERN e^+e^- collider LEP rule out any such extension of the standard model with a light Majoron. We therefore choose not to travel this route but rather have (4) ensuring tree unitarity in the $(WWee)$ four-point amplitude for high values of the WW c.m. energy.

On the other hand, it is entirely possible to have one relatively low-lying heavy Majorana neutrino around a TeV scale while the others are of much higher masses beyond a foreseeable laboratory reach. This is a perfectly natural consequence, for instance, of superstring-generated E_6 models [5]. In the **27** of E_6 there are two more neutral Majorana leptons (N and N') per generation apart from the standard neutrino. These have different transformation properties under the SO (10) subgroup of E_6, one being in the **16** and the other in the singlet **1**. They could naturally have widely different masses depending on the pattern and scales of E_6-symmetry breakdown. In the left-right-symmetric models [6], a Majorana neutrino, which is a singlet under $SU(2)_L\times U(1)_Y$, has a mass which is a Yukawa coupling times the $SU(2)_R$-breaking scale. If the latter is reasonably expected [7] to be in the region of tens of TeV, the Majorana neutrino mass could very well be around a TeV. A heavy fourth-generation Majorana neutrino has also been proposed [8].

Without commitment to any specific model, let us assume the existence of one such heavy Majorana neutrino N_e with a mixing factor U_{eN} and a Majorana mass M in and around the TeV scale. Furthermore, all the other N_{ej}, needed to satisfy (4), are taken to be much heavier. Since the Majorana mass eigenvalue of the highest physical electron neutrino is known [2] to be below a few eV, for effects at subprocess energies in and around a TeV, we need to consider the diagrams of Fig. 1 for $W^+W^+\to e^+e^+$ exchanging only this N_e. The other N_{ej} ensure tree unitarity at very high energies but effectively decouple from the regime of our interest.

The best source of two positively charged W^*'s (i.e., virtual W's) interacting with c.m. energy near a TeV is a multi-TeV proton-proton collider such as the LHC or SSC. There are three possible subprocesses now: (1) two identical valence d quarks from the colliding protons can scatter into a state carrying lepton number $+2$: $dd\to\bar{u}\,\bar{u}W^{+*}W^{+*}\to\bar{u}\,\bar{u}e^+e^+\nu_e\nu_e$; (2) two antiquarks from the two seas could cause the reaction $\bar{d}\bar{d}\to\bar{u}\,\bar{u}W^{+*}W^{+*}\to\bar{u}\,\bar{u}e^+e^+\nu_e\nu_e$; (3) a valence u quark from one proton and a $\bar{d}$ antiquark from the sea of the other could induce the process $u\bar{d}\to d\bar{u}W^{+*}W^{+*}\to d\bar{u}\,e^+e^+\nu_e\nu_e$. It is straightforward to include higher-generation quarks or antiquarks from the sea by inserting the appropriate Cabibbo-Kobayashi-Maskawa factors in their couplings with W^+. These factors add up to unity in the square of the matrix element.

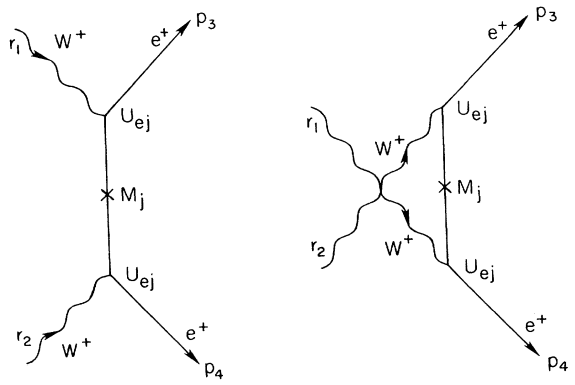

FIG. 1. Tree diagrams for $W^+W^+\to e^+e^+$.

We assign four-momenta $q_{1,2}$ to the two incident quark (antiquark) lines, $p_{1,2}$ to the two final ones, and as before $p_{3,4}$ to the positrons produced. Now the two external W^+ lines of Fig. 1 become two internal W^{+*} lines attached to the external quark (antiquark) lines. It is convenient to define

$$\hat{t}_A\equiv(q_1-p_1-p_3)^2=2(p_1\cdot p_3-q_1\cdot p_1-q_1\cdot p_3)\ ,$$

$$\hat{u}_A\equiv(q_2-p_2-p_3)^2=2(p_2\cdot p_3-q_2\cdot p_2-q_2\cdot p_3)\ ,$$

$$\hat{t}_B\equiv(q_1-p_2-p_3)^2=2(p_2\cdot p_3-q_1\cdot p_2-q_1\cdot p_3)\ ,$$

and

$$\hat{u}_B\equiv(q_2-p_1-p_3)^2=2(p_1\cdot p_3-q_2\cdot p_1-q_2\cdot p_3)\ ,$$

neglecting the quark masses. For either of the modes (1) and (2) there are four Feynman diagrams since one can interchange the final quark (antiquark) lines and effect the changes $\hat{t}_A,\hat{u}_A\leftrightarrow\hat{t}_B,\hat{u}_B$. In contrast, mode (3) allows only two diagrams corresponding to those of Fig. 1 with the W^{+*}'s attached to one external quark and one external antiquark line.

Let $\overline{\sum}$ for "initial-averaged and final-summed" over colors and spins. Furthermore, let a caret on top signify a subprocess and let the subscript refer to the mode discussed above. (We neglect the width in the W propagator.) The invariant matrix-element squared for the three possibilities are then given by

$$\overline{\sum}|\hat{\mathcal{M}}_{1,2,3}|^2=512|U_{eN}|^4\pi^4\alpha_{\rm EM}^4\sin^{-8}\theta_W M^2(2q_1\cdot p_1+M_W^2)^{-2}(2q_2\cdot p_2+M_W^2)^{-2}K_{1,2,3}\ , \tag{5}$$

with

$$K_1 = q_1\cdot q_2\left\{p_1\cdot p_3 p_2\cdot p_4\left[\frac{2}{3}\frac{\hat{u}_A-\hat{t}_A}{(\hat{u}_A-M^2)(\hat{t}_A-M^2)^2}+\frac{1}{6}\left[\frac{1}{\hat{t}_A-M^2}+\frac{1}{\hat{u}_B-M^2}\right]^2\right.\right.$$
$$\left.-\frac{1}{6}\left[\frac{1}{\hat{t}_A-M^2}+\frac{1}{\hat{u}_B-M^2}\right]\left[\frac{1}{\hat{t}_B-M^2}+\frac{1}{\hat{u}_A-M^2}\right]\right]$$
$$+p_1\cdot p_4 p_2\cdot p_3\left[\frac{2}{3}\frac{\hat{t}_A-\hat{u}_A}{(\hat{u}_A-M^2)^2(\hat{t}_A-M^2)}+\frac{1}{6}\left[\frac{1}{\hat{t}_B-M^2}+\frac{1}{\hat{u}_A-M^2}\right]^2\right.$$
$$\left.-\frac{1}{6}\left[\frac{1}{\hat{t}_B-M^2}+\frac{1}{\hat{u}_A-M^2}\right]\left[\frac{1}{\hat{t}_A-M^2}+\frac{1}{\hat{u}_B-M^2}\right]\right]$$
$$\left.+p_1\cdot p_2 p_3\cdot p_4\left[\frac{2}{3}\frac{1}{(\hat{u}_A-M^2)(\hat{t}_A-M^2)}+\frac{1}{6}\left[\frac{1}{\hat{t}_B-M^2}+\frac{1}{\hat{u}_A-M^2}\right]\left[\frac{1}{\hat{t}_A-M^2}+\frac{1}{\hat{u}_B-M^2}\right]\right]\right\} \quad (6)$$

$$K_2 = p_1\cdot p_2\left\{q_1\cdot p_3 q_2\cdot p_4\left[\frac{2}{3}\frac{\hat{u}_A-\hat{t}_A}{(\hat{u}_A-M^2)(\hat{t}_a-M^2)^2}+\frac{1}{6}\left[\frac{1}{\hat{t}_A-M^2}+\frac{1}{\hat{t}_B-M^2}\right]^2\right.\right.$$
$$\left.-\frac{1}{6}\left[\frac{1}{\hat{t}_A-M^2}+\frac{1}{\hat{t}_B-M^2}\right]\left[\frac{1}{\hat{u}_A-M^2}+\frac{1}{\hat{u}_B-M^2}\right]\right]$$
$$+q_1\cdot p_4 q_2\cdot p_3\left[\frac{2}{3}\frac{\hat{t}_A-\hat{u}_A}{(\hat{u}_a-M^2)^2(\hat{t}_A-M^2)}+\frac{1}{6}\left[\frac{1}{\hat{u}_A-M^2}+\frac{1}{\hat{u}_B-M^2}\right]^2\right.$$
$$\left.-\frac{1}{6}\left[\frac{1}{\hat{u}_A-M^2}+\frac{1}{\hat{u}_B-M^2}\right]\left[\frac{1}{\hat{t}_A-M^2}+\frac{1}{\hat{t}_B-M^2}\right]\right]$$
$$\left.+q_1\cdot q_2 p_3\cdot p_4\left[\frac{2}{3}\frac{1}{(\hat{t}_A-M^2)(\hat{u}_A-M^2)}+\frac{1}{6}\left[\frac{1}{\hat{t}_A-M^2}+\frac{1}{\hat{t}_B-M^2}\right]\left[\frac{1}{\hat{u}_A-M^2}+\frac{1}{\hat{u}_B-M^2}\right]\right]\right\}. \quad (7)$$

and

$$K_3 = \frac{q_1\cdot p_2}{(\hat{t}_A-M^2)(\hat{u}_A-M^2)}\left[(\hat{u}_A-\hat{t}_A)\left[\frac{p_1\cdot p_3 q_2\cdot p_4}{\hat{t}_A-M^2}-\frac{p_1\cdot p_4 q_2\cdot p_3}{\hat{u}_A-M^2}\right]+p_1\cdot q_2 p_3\cdot p_4\right]. \quad (8)$$

Equation (5) contains two unknown constants M and U_{eN}. Since M^2 appears in the numerator as well as (in linear combination with $\hat{t}_A$ or $\hat{t}_B$ or $\hat{u}_A$ or $\hat{u}_B$) in the denominators, the cross section is expected to be largest over a finite interval of M and to fall off on both sides of it. We aim to locate this optimal mass interval which can generate a visible signal at LHC and SSC energies. Turning to U_{eN}, experimental bounds on the lack of universality in the $e\bar{\nu}_e W$ coupling imply [9] that $|U_{eN}|^2<0.043$. (Corresponding upper bounds for $|U_{\mu N}|^2$ and $|U_{\tau N}|^2$ are 0.008 and 0.14, respectively, and suggest that it is better to consider dielectrons rather than dimuons in the final state; ditaus are of course inconvenient since they generate missing p_T.) So we use 0.043 for $|U_{eN}|^2$.

To generate our results numerically we convolute the appropriate phase-space integral of the above matrix elements with Duke-Owens parton distribution functions evolved at $Q^2=\hat{s}$ for $\Lambda=0.2$ GeV at pp colliders with $\sqrt{s}=40$ TeV (SSC) and 16 TeV (LHC). In the parton-level Monte Carlo model that we employ for both our signal and background calculations, the formation of hadron jets is simulated solely on the basis of the energy and momenta of the final-state partons. We first order the final-state partons according to their values of p_T. Around the parton of highest p_T we then coalesce into a cluster all partons lying within a cone of

$$\Delta r_{\rm jet}\equiv[(\Delta\eta)^2+(\Delta\phi)^2]^{1/2}<1.0\ , \quad (9)$$

where η is the pseudorapidity and ϕ the azimuthal angle. This process is repeated among the remaining partons until we are left with some number of well-separated clusters. A cluster for the SSC calculations is regarded as a jet if it has $p_T(\text{jet})>30$ GeV and $|\eta_{\rm jet}|<5$. We require our signal to have exactly two jets defined in this way.

We also require the following selection criteria on the two final-state positrons to ensure lepton identification:

$$|\eta_{\rm lep}|<5,\quad p_T(\text{lep})>10\ \text{GeV}\ , \quad (10)$$

and then we apply isolation cuts upon the positrons to help distinguish them from background. This isolation criterion is defined by generating a cone of $\Delta r_{\rm lep} < 1.0$ about each lepton in which we demand that there be no hadronic activity. After these cuts are applied, the resulting cross section is computed and is displayed in Fig. 2 as a function of the Majorana mass of the heavy neutrino M for $\sqrt{s} = 40$ TeV; the cross section for $\sqrt{s} = 16$ TeV is also displayed in this figure. For the LHC calculation, however, we have employed the following lepton isolation and jet definitions:

$$\Delta r_{\rm jet} < 0.5\ ,\quad p_T(\text{jet}) > 20\ \text{GeV},\quad |\eta_{\rm jet}| < 4,$$
$$\Delta r_{\rm lep} > 0.5\ ,\quad p_T(\text{lep}) > 5\ \text{GeV},\quad |\eta_{\rm lep}| < 4\ . \tag{11}$$

At the SSC the optimal mass interval of M is found to lie between 450 GeV and 1700 GeV, for which the cross section varies between 0.20 and 0.23 fb. (The cross section without cuts is approximately twice this size.) For the anticipated integrated SSC luminosity, $\mathcal{L} = 10$ fb^{-1}/yr, this corresponds to a very small event rate of two events per year. The same event rate may be had at the LHC over a slightly broader mass interval of 150 GeV $< M <$ 1400 GeV, but only for a luminosity of 10^{34} cm^{-2}/s or 100 fb^{-1}/yr. At lower values of $\sqrt{s}$, the cross section drops quickly and a measurable event rate cannot be realized for any optimized mass interval of M; this is because the subprocess involves the WW interaction which becomes significant only for $\sqrt{s}$ in the multi-TeV region.

There are two main sources of standard-model background that can mimic our signal. First, the reaction $pp \to (\text{jet})_1(\text{jet})_2 W^+W^+$, where each W^+ subsequently decays to $e^+\nu_e$, is one contender when the sum of the transverse momenta of the two ν_e's is small. The corresponding subprocesses are $uu \to ddW^+W^+$, $u\bar{d} \to d\bar{u}W^+W^+$ and $\bar{d}\,\bar{d} \to \bar{u}\,\bar{u}W^+W^+$ and similar ones with higher-generation quarks or antiquarks. In fact, two classes of Feynman diagrams contribute here: (a) those with a gluon-mediated QCD scattering between the quarks/antiquarks followed by the emission of two real W^+'s [10], and (b) those in which the quarks/antiquarks emit two virtual W^{+*}'s, which then scatter into two real W^+'s [11]. The two contributions are incoherent because of color. Contribution (b) depends on an unknown Higgs-boson mass but is not numerically sensitive to that. We have calculated the total cross section, including both contributions plus spin correlation effects for the subprocesses $uu \to dd\,e^+e^+\nu_e\nu_e$, $u\bar{d} \to d\bar{u}e^+e^+\nu_e\nu_e$, and $\bar{d}\,\bar{d} \to \bar{u}\,\bar{u}e^+e^+\nu_e\nu_e$. We impose a "$\mathbf{p}_T$-conservation" condition by requiring that the x and y components of neutrino momenta separately satisfy

$$\left| \sum_{\nu_i} p_{ix} \right| \le \eta \sum_{\nu_i} |p_{ix}| \tag{12}$$

for which we allow an uncertainty in p_T determination of $\eta = 0.02$. We employ also the jet definition and lepton cuts outlined in the discussion of the signal above, to obtain the final $pp \to (\text{jet})_1(\text{jet})_2 e^+e^+$ cross section. Both for LHC and SSC energies, this background cross section turns out to be 10^{-2} fb, well below our signal level. The background reduction is overwhelmingly due to the "$\mathbf{p}_T$-conservation" condition and the requirement of a maximum 2% uncertainty in p_T determination is crucial.

The second main source of background is due to $t\bar{t}$ production, which can result in events containing same-sign dileptons and jets when one t decays to bW^+, $W^+ \to e^+\nu$, and the $\bar{t}$ decays to $\bar{b}W^-$, $\bar{b} \to \bar{c}e^+\nu$, $W^- \to qq'$. (A comparable background could arise from the formation of T and $\bar{T}$ mesons and T and $\bar{T}$ mixing, but we do not consider it here because of the uncertainties of T formation for a heavy top quark and of the mixing angle.) At the SSC for $m_t = 100$ GeV, for example, the raw rate for production of $t\bar{t}$ pairs, multiplied by the appropriate branching fractions, yields 4×10^6 positron pairs per year, an overwhelming rate in comparison to our signal. Nevertheless we can demonstrate here that it is possible, by requiring these events to have other characteristics in common with our signal, to drastically reduce this enormous background-event sample. In particular we find that the most effective of the cuts are those limiting the $\not{p}_T$ of each event, because of the unlikelihood that the p_T of each neutrino will cancel, and of lepton isolation. The effectiveness of the latter is due to the fact that one of the two dileptons must result from the secondary decay of the b quark, whose decay products tend to be highly collinear. For this same reason, we need not consider the background contributions due to $b\bar{b}$ and $c\bar{c}$ pairs; we expect all such events to be easily cut from the event sample by requiring lepton isolation.

We calculate the rate for $t\bar{t}$ production, from gluon and quark initial states at the SSC for $m_t = 100$ GeV, and the subsequent decay to the seven-particle final state $(be^+\nu)(\bar{c}e^+\nu)(qq')$. In our calculation no spin correlation effects are included as we expect [12] these to be small. We submit the final-state partons to the same jet-counting algorithm described above and cut from the

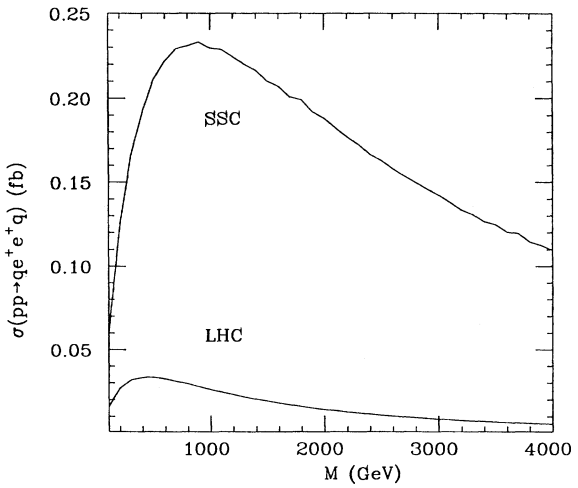

FIG. 2. Signal cross section as a function of the heavy Majorana neutrino mass M at the SSC and at the LHC with cuts as described in text.

background sample all those events which do not have exactly two jets such that $\Delta r_{\rm jet} < 1.0$, $|\eta_{\rm jet}| < 5.0$, and $p_T({\rm jet}) > 30$ GeV. We require that each positron have $p_T({\rm lep}) > 10$ GeV and that it be free of hadronic activity within cones of $\Delta r_{\rm lep} = 1$. Finally we demand the "$\mathbf{p}_T$-conservation" requirement of Eq. (12). In our worst-case scenario for which $m_t = 125$ GeV, in that $t\bar{t}$ production is most copious, we find the background-event sample falls exponentially as η is decreased and is approximately given by

$$\sigma = \sigma_0 \exp(-a\eta^{-b}) , \tag{13}$$

where $\sigma_0 = 5.0 \times 10^3$ fb, $a = 0.28$ and $b = 0.81$. Thus the background is a sensitive function of how accurately the condition (12) can be implemented and falls below 0.10 fb only for η less than 0.011. For other top mass values η can be slightly larger; if $m_t = 100$ GeV, η needs to be less than 0.015, whereas η could be 0.013 if m_t turns out to be close to 200 GeV.

At the LHC we find the heavy flavor background even more difficult to eliminate. For the jet definition and set of cuts we have chosen specific to the LHC [Eq. (11)], same-sign dilepton production from $t\bar{t}$ pairs of mass 100 GeV persists at the rate of 1.7 fb for a $\not{p}_T$ measurement uncertainty $\eta = 0.01$. This decreases only to about 1 fb for $m_t = 125$ GeV. For $m_t = 200$ GeV, this rate is still 0.03 fb for $\eta = 0.01$, which lies above our signal rate for almost all mass values of the heavy Majorana neutrino.

We have considered a specific source of electron number violation via a heavy electron-type Majorana neutrino coupling to the electron through a standard W gauge boson with a mixing angle [13] of 0.2, the maximum permitted by present data. Within this scenario, we show that the signal process $pp \to ({\rm jet})_1({\rm jet})_2 e^+ e^+$ may probe the heavy Majorana mass interval 450–1700 GeV at the SSC for the design luminosity $\mathcal{L} = 10$ fb^{-1}/yr, as well as the mass interval 150–1400 GeV at the LHC for $\mathcal{L} = 100$ fb^{-1}/yr at a rate of two events per year. We have also shown that in spite of the extremely small rates of our signal, the major sources of standard-model background may possibly be cut from the event sample at the SSC by requiring lepton isolation and limiting the amount of $\not{p}_T$. At the LHC it is not possible, with our cuts, to suppress the background sufficiently. Of course, there could exist other sources of electron number violation beyond the standard model that could mimic our signal. These include the analog of this process mediated by right-handed W's, the Drell-Yan production of right-handed W's with subsequent decay to same-sign lepton pairs and jets [14], or R-parity-breaking interactions in a supersymmetric extension [15], but we consider none of these possibilities here.

We thank H. Baer, V. Barger, T. G. Rizzo, and especially X. R. Tata for helpful discussions. Computing resources were provided in part by the University of Texas Center for High Performance Computing. This research has been supported in part by the U. S. Department of Energy Grant No. DE-FG05-85ER40200.

*Permanent address: Tata Institute of Fundamental Research, Bombay, India.

[1] E. Majorana, Nuovo Cimento **14**, 171 (1937). W. H. Furry, Phys. Rev. **54**, 56 (1938); P. D. Mannheim, Int. J. Theor. Phys. **23**, 643 (1984); B. Kayser, Commun. Nucl. Part. Phys. **14**, 64 (1985); H. E. Haber and G. L. Kane, Phys. Rep. **117**, 76 (1987).

[2] M. Doi, T. Kotani, and E. Takasugi, Prog. Theor. Phys. Suppl. **83**, 1 (1985); S. M. Bilenky and S. T. Petcov, Rev. Mod. Phys. **59**, 671 (1987).

[3] T. G. Rizzo, Phys. Lett. **116B**, 23 (1982).

[4] H. M. Georgi, S. L. Glashow, and S. Nussinov, Nucl. Phys. **B193**, 297 (1981); V. Barger *et al.*, Phys. Rev. D **26**, 218 (1982).

[5] J. L. Hewett and T. G. Rizzo, Phys. Rep. **183**, 193 (1989).

[6] J. C. Pati and A. Salam, Phys. Rev. D **10**, 275 (1974).

[7] R. N. Mohapatra, in *CP Violation,* edited by C. Jarlskog (World Scientific, Singapore, 1988).

[8] C. T. Hill and E. A. Paschos, Phys. Lett. B **247**, 96 (1990).

[9] H. E. Haber and M. H. Reno, Phys. Rev. D **34**, 2732 (1986); M. Gronau, C. N. Leung, and J. L. Rosner, *ibid.* **29**, 2539 (1984).

[10] D. A. Dicus and R. Vega, Phys. Lett. B **217**, 194 (1989).

[11] R. Vega and D. A. Dicus, Nucl. Phys. **B329**, 533 (1990).

[12] V. Barger, J. Ohnemus, and R. J. N. Phillips, Int. J. Mod. Phys. A **4**, 617 (1989).

[13] For any "natural" mixing mechanism one would expect a relation between the mixing angle and the mass ratio. Since our mass ratio is of order 10^9, a natural mixing angle would be of order 10^{-4} and our clean but small signal would disappear. Thus the observation of such a signal would present a theoretical challenge to model builders. We are concerned here with what it is possible to observe rather than what seems likely from theoretical prejudice, but we thank Lincoln Wolfenstein for emphasizing this point to us.

[14] W.-Y. Keung and G. Senjanović, Phys. Rev. Lett. **50**, 1427 (1983).

[15] L. J. Hall, Mod. Phys. Lett. A **5**, 467 (1990), and references therein.